Superconducting transitions in $Hg_{3-\delta}SbF_6$

P. A. P. Laroche and W. R. Datars
Department of Physics, McMaster University, Hamilton, Ontario, Canada L8S 4M1
(Received 10 September 1986)

$Hg_{3-\delta}SbF_6$ exhibits two distinct superconducting transitions in magnetization measurements: one at 3.7 K and one at 0.42 K with the field parallel to the c axis. The high-temperature transition at 3.7 K has a partial Meissner effect and a critical field near 400 G. The low-temperature transition at 0.42 K has a complete Meissner effect and a critical field of 15.4 G. In between these two transitions is a region where flux exclusion increases approximately linearly with decreasing temperature at a rate of 0.17 G/K for an applied field of 10.9 G. The flux exclusion is approximately 7% of complete flux exclusion at the onset of the low-temperature transition. The high-temperature transition is due to bulklike mercury regions containing less than 2% of the entire mercury in the sample. Superconductivity at the low-temperature transition is intrinsic to the compound.

I. INTRODUCTION

$Hg_{3-\delta}SbF_6$ is one member of a family of compounds of the form $Hg_{3-\delta}XF_6$; X=Sb, As, Nb, and Ta. The Sb and As compounds were studied first and have received considerable attention because Hg atoms lie in mutually perpendicular chains in the crystallographic a-b plane implying that one-dimensional or two-dimensional effects should be observed.

The $Hg_{3-\delta}SbF_6$ compound has been investigated by neutron and x-ray diffraction,[1] resistivity,[2] reflectivity,[3] differential thermal analysis,[4] and cooling rate effects on resistivity and magnetic susceptibility.[5] These experiments have established a strong two-dimensional dependence of the sample which is illustrated best by the Fermi surface obtained by de Haas–van Alphen experiments.[6] They also show that the mercury chains order as samples are cooled and that bulk like mercury is present in the sample at low temperatures.

The present work uses dc magnetization measurement in the 0.1–4.0-K temperature range to observe superconductivity in $Hg_{3-\delta}SbF_6$. Since Hg is the only superconducting element in this compound, this system provides a distribution of a superconducting element in a nonsuperconducting matrix. However, all the Hg atoms are not necessarily in ordered chains as shown by differential thermal analysis.[4] It is the aim of the present investigations to characterize the superconductivity that arises from such a distribution and to elucidate as much as possible the effects observed.

The superconductivity of $Hg_{3-\delta}AsF_6$ has been studied extensively. Superconductivity with a partial Meissner effect below 4 K has been attributed to mercury dispersed in isolated regions of the crystal.[7,8] However, resistivity and susceptibility measurements by Batalla and Datars[9] show that this superconductivity is not one dimensional as reported by Chiang *et al.*[10] Meissner effect data indicates that the superconductivity of $Hg_{3-\delta}AsF_6$ goes to complete flux exclusion below 0.4 K.[11,12]

II. EXPERIMENTAL PROCEDURE

Measurements were made with a superconducting quantum interference device (SQUID) magnetometer. The magnetometer coils were wound on a hollow, copper foil form. It was placed in a copper body which was attached directly to the bottom of the mixing chamber of a dilution refrigerator. The sample temperature, which was varied between 0.1 and 4 K, was determined by a calibrated carbon resistance thermometer mounted on the mixing chamber and by a germanium thermometer mounted into the copper magnetometer body.

Four 14-turn, pick-up coils formed a double gradient system in the magnetometer with a Helmholtz separation between the central pair of coils. The sample was mounted between the middle pair of coils. The four coils were wound with superconducting wire of diameter 0.7 mm and were connected directly to a SQUID mounted in the He^4 bath. The magnetic field at the sample was generated by a 3100-turn superconducting solenoid wound on the outside of the copper body of the magnetometer.

The magnetization measurements were conducted on three crystals of $Hg_{3-\delta}SbF_6$ and a piece of tin. The $Hg_{3-\delta}SbF_6$ crystals were picked from many samples for their uniform crystal growth. The tin sample was shaped to reproduce as accurately as possible the dimensions of a crystal with a volume of 3.57×10^{-4} cm^3.

One crystal was sealed in a plastic sample holder, in a dry box, so that the c axis was parallel to the applied magnetic field when placed in the magnetometer. The other crystals, for which a tin sample of similar shape was not examined, were used with the c axis perpendicular to the applied magnetic field.

The piece of tin, a type-I superconductor with $H_c(0)=305$ G and $T_c=3.72$ K, was used to calibrate the field current and the SQUID magnetometer output. The magnetization of tin followed the expected behavior of increasing linearly with increasing applied field up to $(1-n)H_c$, where $1-n$ depends on the shape of the sam-

ple and then decreasing linearly with further increase in field up to H_c where the entire superconductor becomes normal.[13] The Bardeen-Cooper-Schrieffer (BCS) equations for superconductivity were used to calculate the critical field from $H_c(0)$ and T_c and hence calibrate the field current. This field was within 1% of that predicted at the center of the solenoid from the relationship between magnetic field and current for a solenoid. For fields less than $(1-n)H_c$, the magnetization calibration was $(1-n)^{-1}$ times the applied magnetic field at the tin sample where $1-n$ was 0.342 for our tin sample.

III. RESULTS

Magnetization for the temperature range 1.0 to 4.0 K is shown in Fig. 1 for a set of magnetic fields with the field parallel to the c axis. The data are shown for cooling in magnetic fields of 4.6, 7.8, and 9.0 G and warming in fields of 2.7 and 10.9 G applied at the beginning of the warming cycles. In each case partial flux exclusion increases with decreasing temperature over the entire temperature range. The shift in T_c between the curves is largely due to hysteresis caused by a small difference in temperature between the sample and the thermometer and, to a lesser extent, to the magnetic field dependence of T_c. The zero-field T_c of the high-temperature transition obtained from the mean is 3.7 K.

Magnetization curves for the $Hg_{3-\delta}SbF_6$ sample are shown in Fig. 2 for 0.1 to 4.0 K. The continuous curve over the entire temperature range was taken during warming with a field of 10.9 G applied at 0.1 K. The other curves are cooling curves through the low-temperature transition only.

The cooling curves show a magnetization that becomes increasingly diamagnetic with decreasing temperature down to the low-temperature transition. Therefore, the fraction of flux exclusion increases with decreasing temperature. The high temperature transition gives a small partial flux exclusion reaching a few percent before the low-temperature transition. The warming curve at 10.9 G shows 7% flux exclusion above the low-temperature transition. The magnetic field dependence of the transition is similar to that of $Hg_{3-\delta}AsF_6$ for which the critical field is about 400 G.

The low-temperature transition is shown in an expanded view in Fig. 3. It appears as a transition going from the linearly increasing region. Unlike the high-temperature transition that displays a very small change in T_c from 0 to 11 G, the T_c of the low-temperature transition is depressed by a few tenths of a kelvin over the same field range. This indicates that the low-temperature transition has a low critical field.

Magnetization *versus* field at 0.23, 0.26, 0.29, 0.32, 0.36, 0.43, and 0.56 K is plotted in Fig. 4 over the field range 0 to 11 G. The low-temperature transition rises up

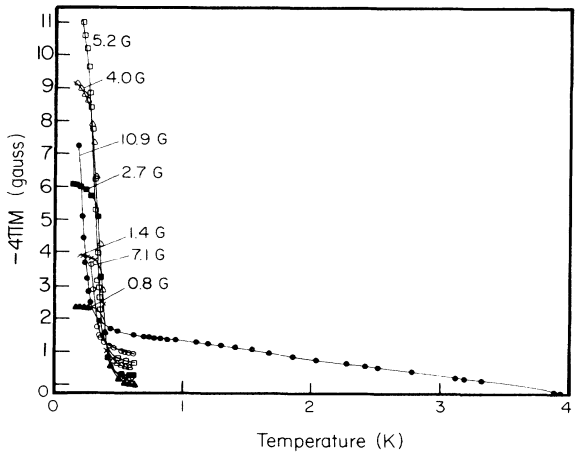

FIG. 2. Temperature dependence of the magnetization with the field parallel to the c axis of $Hg_{3-\delta}SbF_6$ for temperatures above 0.1 K. The 10.9-G curve is a warming curve and the others are cooling curves.

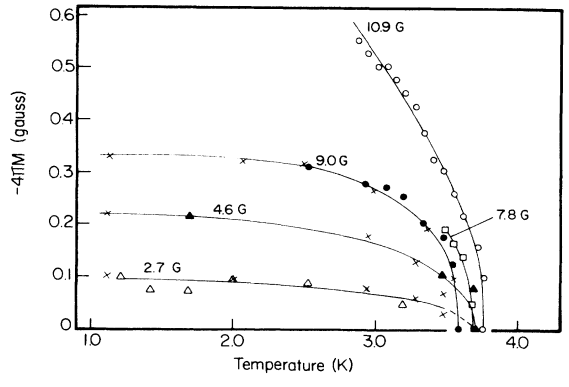

FIG. 1. Temperature dependence of the magnetization of $Hg_{3-\delta}SbF_6$ between 1 and 4 K for different applied magnetic fields with the field parallel to the c axis. The solid lines are for the penetration depth model for small regions with $r/\lambda_0=4$; $\lambda_0=10^{-4}$ m; $T_c=3.7$ K.

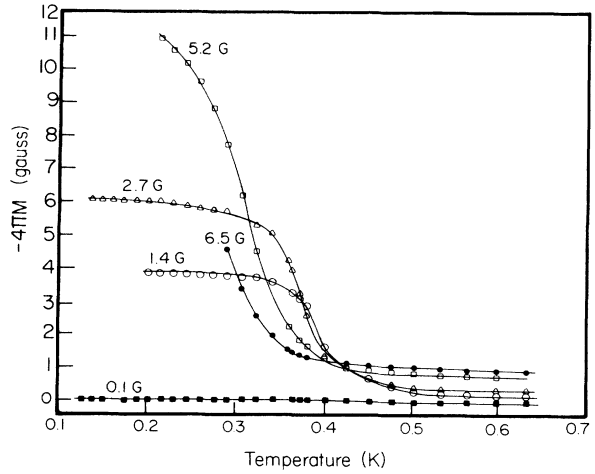

FIG. 3. Temperature dependence of the magnetization of $Hg_{3-\delta}SbF_6$ through the low-temperature transition for different applied magnetic fields parallel to the c axis.

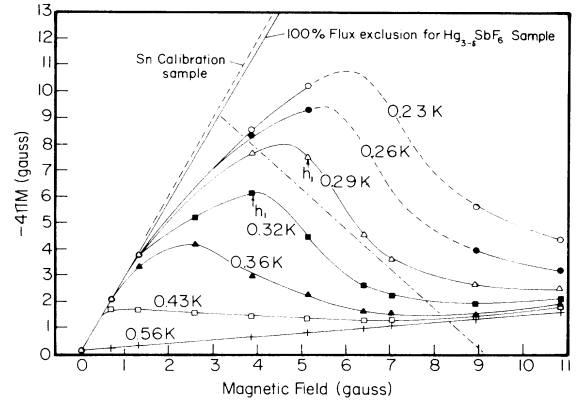

FIG. 4. Magnetic field dependence of the magnetization with the field parallel to the c axis of $Hg_{3-\delta}SbF_6$ for temperatures between 0.23 and 0.56 K. The dashed line indicates measurements of a Sn calibration sample and h_1 is the predicted critical field at the onset of the intermediate state.

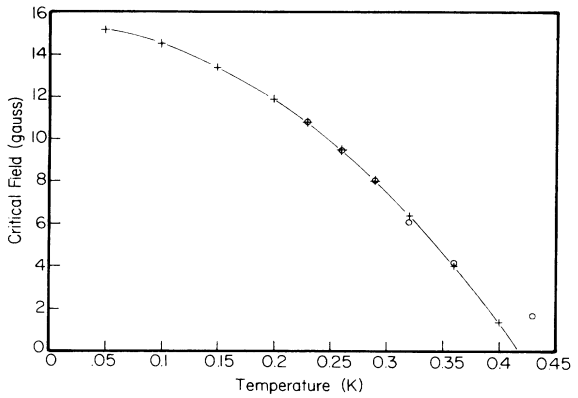

FIG. 5. Critical field of the low-temperature transitions of $Hg_{3-\delta}SbF_6$. The solid line is calculated from BCS theory with $T_c = 0.42$ K and $H_c = 15.4$ G. The crosses are calculated values and the circles are measured values.

from the high-temperature transition which forms the background level shown by the 0.56-K data. The dashed line shows the Sn 100% flux exclusion line; the dotted line shows the bulk demagnetization of the Hg sample expected from the shape. The agreement between the initial slope of the Hg sample and the Sn sample is better than 4% showing that the low-temperature transition is a bulk transition.

The general shape of the curves in Fig. 4 is due to the geometry of the sample. The results of Landau's intermediate state model applied to thin disks by Andrew and Lock[13] are used to approximate the present thin plate geometry. The model predicts that the intermediate state will begin at $h_1(T)$. Estimations of $h_1(T)$ with the procedure of Andrew and Lock are 4.1 and 5.1 G for 0.32 and 0.29 K, respectively. Figure 5 is a plot of critical field *versus* temperature. The critical fields were determined from the magnetization maxima. The zero field T_c was found to be 0.42 K. A least-squares fit of the BCS equation was done and plotted. The BCS $H_c(0)$ is 15.4 G which is much smaller than that of the high-temperature transition. The critical field deviated from the BCS prediction for temperature near T_c.

Two samples were studied with the magnetic field perpendicular to the c axis. However, there is no calibration with tin samples of similar shape so that the demagnetization factors for the samples are not known. Again, there are superconducting transitions below 4.0 K and below 0.5 K. However, the change in magnetization at the high-temperature transition is approximately 7% of that at the low-temperature transition in one sample while in the other sample the change in magnetization is 2 orders of magnitude smaller at the high-temperature transition than at the low-temperature transition. The first sample is similar to the sample with the field parallel to the c axis. The small superconductivity at the high-temperature transition in the second sample may be a consequence of how the sample was cooled from room temperature. The low-temperature transition moves to lower temperatures with increasing magnetic field in a way that is similar to that shown in Fig. 3 for the magnetic field parallel to the c axis. This indicates that the critical field and temperature are similar for the two directions of magnetic field.

IV. DISCUSSION

$Hg_{3-\delta}SbF_6$ exhibits two distinct superconducting transitions, one at 3.7 K and one at 0.42 K. The high-temperature transition at 3.7 K has a partial Meissner effect and a critical field near 400 G. The low-temperature transition at 0.42 K has a complete Meissner effect and a critical field of 15.4 G. In between these two transitions is a region where flux exclusion decreases approximately linearly with increasing temperature at a rate of 0.17 G/K for an applied field of 10.9 G during warming. The flux exclusion is approximately 7% of complete flux exclusion at the onset of the low-temperature transition.

Magnetization curves show the presence of the high-temperature-transition flux exclusion as a background level for the low-temperature transition. Bulk superconductivity is evident from the initial slope of $-4\pi M$ versus H of the low-temperature transition which follows the behavior of the Sn calibration sample. Departure from the Sn magnetization is observed as a rounding off of the linear $-4\pi M$ versus H line with increasing field and the formation of a tail which merges into the high temperature transition background.

The high-temperature transition has a critical field similar to the bulk critical field of Hg and a critical temperature that is a few tenths of a kelvin below the critical temperature of free mercury. This implies that the high-temperature transition results from bulklike mercury. The partial flux exclusion associated with this transition reaches a maximum of 7% of complete flux exclusion. Therefore only a fraction of the mercury present in the sample participates in the formation of the bulklike mercury regions.

As the first regions superconduct at 3.7 K, the slope of the $\Delta(-4\pi M)/\Delta H$ versus T curve approaches infinity. At 3.6 K, the rate of growth with temperature reduces to approximately -0.022 K^{-1} and levels off to approxi-

mately $-0.013\ K^{-1}$ at 2.5 K. The amount of flux exclusion associated with the high-temperature transition can be used to estimate the percentage of bulklike mercury in the sample.

The following points are assumed.

(1) The Hg that contributes to the nearly free mercury transition is identical to α Hg.

(2) The smallest dimension of a region is equal to a typical penetration depth 10^{-7} m.

(3) The mercury regions are spherical.

(4) Superconductivity occurs exclusively in mercury regions.

We then determine the following:

(5) The number of Hg atoms in a spherical region of radius r which equals the penetration depth.

(6) The magnetic moment of a single sphere following Plonus.[14]

(7) The sum of the magnetic moments of all the spheres and divide by the sample volume to get the magnetization of the sample.

(8) Finally, we relate the percentage of the total mercury in the sample that is in the spherical regions of the sample to the magnetization.

We find that $-4\pi M/H$ increases linearly from zero with increasing percentage of mercury and is equal to 0.32 when there is 2% of the total mercury of the sample in spheres. This compares with the observed value of $\Delta(-4\pi M)/\Delta H$ at 3.4 K, the temperature at which supercooling and superheating effects are not important although they are expected to become evident for our sample size at lower temperatures.[15] One concludes that less than 2% of the total amount of mercury in the sample contributes to the high-temperature transition. The percentage of mercury is very similar to the amount of bulk mercury observed in differential thermal analysis experiments[4] implying that the same mercury is observed. A model[16] for the change of penetration depth with temperature for small regions fits the data of Fig. 1 for $r/\lambda_0=4$, with a penetration depth $\lambda_0=10^{-5}$ cm and $T_c=3.7$ K. The effective radius r of the superconducting regions is a very rough estimate of the size of such regions as the regions are likely distributed over a large range of sizes and shapes including multiply connected regions. As a consequence of these small regions, one would expect supercooling and superheating effects below 3.4 K.[15] This is indicated because the warming curve at 10.9 G shows considerably more excluded flux below 3.4 K than does the cooling curves.

Little is known about the exact nature of the observed mercury-like regions in the linear chain compounds. Spal *et al.*[11] used x-ray fluorescence to show that carefully handled $Hg_{3-\delta}AsF_6$ samples have little or no surface mercury. Mercury is likely inside the sample because the observed T_c is always lower than that of free mercury. Several authors have suggested that the mercury is in defects or cracks.[7,8]

The low-temperature transition shows a complete Meissner effect. The general shape of the magnetization curve agrees qualitatively with the Landau intermediate state model applied to a thin plate. The low critical field and the qualitative agreement with the intermediate state model are indicative of type-I superconductivity.

The tail in Fig. 4 may result from coupling between the intrinsic superconductor and the mercury-like regions. This may also cause the increased critical field observed near the T_c of the low-temperature transition (Fig. 5).

This family of compounds is generally classed as anisotropic. The results for the magnetization with field applied parallel and perpendicular to the c axis show that the two transitions are similar. However, the present data are insufficient to establish any isotropic or anisotropic relationship in the superconductivity for the two orientations.

V. CONCLUSIONS

$Hg_{3-\delta}SbF_6$ has two distinct superconducting transitions at 3.7 and 0.42 K with $H_c(0)=400$ and 15.4 G, respectively, and a region between the transitions where a small increase of flux exclusion takes place with decreasing temperature. The high-temperature transition is due to bulklike mercury regions. It is estimated that less than 2% of the entire mercury in the sample participates in these regions. The exact nature of these regions is unknown.

Superconductivity at the low-temperature transition is intrinsic to the compound. The shape of the magnetization-field curve is accounted for by applying Landau's intermediate state model to a thin plate.[13] The low critical field and the qualitative agreement with Landau's intermediate state model indicate that this is type-I superconductivity. The increase in critical field near the T_c of the low-temperature transition, and the tail observed in the magnetization versus temperature curves for the low-temperature transition may be due to coupling between the intrinsic superconductivity of the compound and the mercury-like regions.

ACKNOWLEDGMENTS

The research was supported by the Natural Sciences and Engineering Research Council of Canada. Thanks are extended to Dr. P. K. Ummat for preparing the samples and to Dr. K. Lushington for assistance with operation of the dilution refrigerator.

[1]Z. Tun and I. D. Brown, Acta Crystallogr. B **38**, 2321 (1982).

[2]B. D. Cutforth, W. R. Datars, A. van Schyndel, and R. J. Gillespie, Solid State Commun. **21**, 377 (1977).

[3]E. S. Koteles, W. R. Datars, B. D. Cutforth, and R. J. Gillespie, **20**, 1129 (1976).

[4]W. R. Datars, A. van Schyndel, J. S. Lass, D. Chartier, and R. J. Gillespie, Phys. Rev. Lett. **40**, 1184 (1978).

[5]F. S. Razavi, P. Ummat, and W. R. Datars, J. Phys. F **16**, 61

(1986).
[6]E. Batalla, F. S. Razavi, and W. R. Datars, Phys. Rev. B **25**, 2109 (1982).
[7]J. E. Schirber, A. J. Heeger, and P. Nigrey, Phys. Rev. B **26**, 6291 (1982).
[8]E. Batalla and W. R. Datars, Solid State Commun. **45**, 225 (1983).
[9]E. Batalla and W. R. Datars, Can. J. Phys. **60**, 1348 (1982).
[10]C. K. Chiang, R. Spal, A. M. Denenstein, A. J. Heeger, N. D. Miro, and A. G. MacDiarmid, Solid State Commun. **23**, 243 (1977).
[11]R. Spal, C. E. Chen, A. Denenstein, A. R. McGhie, A. J. Heeger, and A. G. McDiarmid, Solid State Commun. **32**, 641 (1979).
[12]F. Gross, H. Veith, K. Andres, M. Weger, and A. G. McDiarmid, Phys. Rev. B **34**, 3503 (1986).
[13]E. R. Andrew and J. M. Lock, Proc. Phys. Soc. London Sect. A **63**, 13 (1950).
[14]M. A. Plonus, *Applied Electromagnetics* (McGraw-Hill, New York, 1978), p. 329.
[15]A. B. Pippard, Philos. Mag. **43**, 273 (1952).
[16]J. G. Daunt, A. R. Miller, A. B. Pippard, and D. Shoenberg, Phys. Rev. **74**, 842 (1948).